Astron. Astrophys. 328, L9–L12 (1997)

ASTRONOMY AND ASTROPHYSICS

LETTER

Letter to the Editor

ISOCAM 7 micron deep survey of the Lockman Hole: A mid-infrared search for primeval galaxies⋆

Y. Taniguchi[1], L.L. Cowie[2], Y. Sato[1,3], D.B. Sanders[2], K. Kawara[4], R. Joseph[2], H. Okuda[5], C.G. Wynn-Williams[2], T. Matsumoto[5], K.C. Chambers[2], K. Wakamatsu[6], F.X. Désert[7], Y. Sofue[4], and H. Matsuhara[8]

[1] Astronomical Institute, Tohoku University, Aoba, Sendai 980-77, Japan
[2] Institute for Astronomy, University of Hawaii, 2680 Woodlawn Drive, Honolulu, HI 96822, USA
[3] ISO Science Operations Centre, Astrophysics Division of ESA, Villafranca, E-28080 Madrid, Spain
[4] Institute of Astronomy, University of Tokyo, 2-21-1 Osawa, Mitaka, Tokyo 181, Japan
[5] Institute of Space and Astronautical Science, Yoshinodai, Sagamihara, Kanagawa 229, Japan
[6] Department of Technology, Gifu University, 1-1 Yanagido, Gifu 501-11, Japan
[7] Institut d'Astrophysique Spatiale, F-91405 Orsay, France
[8] Department of Physics, Nagoya University, Furo, Chikusa, Nagoya 464, Japan

Received 12 August 1997 / Accepted 11 September 1997

Abstract. We present results of our 7 μm deep survey program made with ISOCAM, the infrared camera of ISO (Infrared Space Observatory). We have found 15 sources above a 5 $\sigma_{\rm rms}$ significance in a small selected area ($3' \times 3'$) in the Lockman HI hole. Among the 15 sources, 14 objects have also been observed in the near infrared (NIR: $\sim$ 2 μm). The majority of the 7 μm sources (11 objects) have NIR counterparts most of which are considered to be galaxies with intermediate redshifts. It is, however, intriguing that two 7 μm sources have no NIR counterpart. These objects may be heavily reddened populations which have not been detected by existing optical and NIR deep surveys.

Key words: galaxies: infrared emission – active galactic nuclei: infrared emission

1. Introduction

When and how did galaxies form? In order to understand this important problem in astrophysics, many observational studies have been conducted so far (e.g., Fukugita, Hogan, & Peebles 1996; Ellis 1997). Since there are many massive galaxies in the local universe, one of the most important issues is to find their progenitors at high redshifts. A striking recent discovery is the detection of CO emission from the quasar BR 1202−0725 at redshift 4.69 (Ohta et al. 1996; Omont et al. 1996). Although there is some ambiguity in the estimate, the molecular gas mass is estimated to be of order $10^{10-11} M_\odot$ which is almost comparable with that of the stellar mass in present-day luminous galaxies. Another exciting discovery was reported by Steidel et al. (1996a,b) who succeeded in detecting spheroidal forming galaxies at $z \simeq$ 3 - 3.5 utilizing the technique for searching Lyman limit galaxies suggested by Cowie (1988). The star formation rates estimated for these galaxies are $\sim 10 M_\odot$ y^{-1}, being high enough to form the number of stars in typical elliptical galaxies. Cowie et al. (1995, 1996) also found a number of massive star-forming galaxies at $1 < z < 1.6$ among their magnitude-limited faint galaxy samples. These observational results encourage us to search for massive primeval galaxies at high redshifts.

Deep survey observations in the optical are powerful for detecting very faint sources in the high-z universe (Tyson 1988; Williams et al. 1996; Lanzetta et al. 1996; Steidel et al. 1996a,b). The observed surface density of such high-z star forming galaxies may, however, be smaller than the value expected from the local density of luminous galaxies (e.g., Lanzetta et al. 1996; Steidel et al. 1996b) and it is possible that we are missing classes of objects with substantial reddening and have not yet sampled fully the high-z counterparts of typical nearby galaxies. Since the nearby, well evolved galaxies consist of old low-mass stars, it is important to find galaxies with numerous low-mass stars.

Send offprint requests to: Y. Taniguchi

⋆ Based on observations with ISO, an ESA project with instruments funded by ESA Member States (especially the PI countries: France, Germany, the Netherlands, and the United Kingdom) and with the participation of ISAS and NASA.

These stars emit their energy from the optical to NIR mostly, implying that they are more luminous in the NIR and MIR (mid-infrared) than in the optical if they were present at high redshifts. This argument verifies the relative importance of deep survey in the infrared (e.g., Cowie et al. 1990, 1994, 1996; Djorgovski et al. 1995). Another concern is that forming galaxies might be heavily reddened. If we take the so-called galactic wind model for elliptical galaxies proposed by Arimoto & Yoshii (1987), it should be remembered that the forming phase before the galactic winds could be heavily obscured by abundant gas and dust inside the system. If these galaxies were commonly present at high redshifts, they can never been found by the existing deep optical and NIR surveys because of the heavy extinction in the rest-frame ultraviolet and optical wavelength regions. However, if we perform a very deep survey in the MIR, it is possible to detect such high-z reddened populations (Taniguchi et al. 1994). At present, only ISO (Kessler et al. 1996) allows us to perform such a deep survey in the MIR. In this *Letter* we present the first results from the deep survey program at 7 μm which was made as a Japan-US (Institute for Astronomy, University of Hawaii) joint project (Taniguchi et al. 1997).

2. Observations and data reduction

Our target field is selected in the Lockman HI hole because the Galactic HI column density, $\sim 4 \times 10^{19}$ cm^{-2}, is the lowest value found over the entire sky, providing the best cosmological window for any extragalactic deep survey observations (Lockman, Jahoda, & McCammon 1986; Jahoda, Lockman, & McCammon 1990). After examining IRAS far-infrared maps, we selected two small fields; LH-NW and LH-SW. Our final target field is LH-NW whose center position is $\alpha(2000) = 10^{\rm h}$ $33^{\rm m}$ $55.5^{\rm s}$ and $\delta(2000) = 57^\circ$ $46'$ $18''$. A deep mid-infrared (5 μm - 8.5 μm) image of the LH-NW field was obtained by the Infrared Space Observatory (ISO: Kessler et al. 1996) on March 26 and 27, 1996 (Revolutions 130 and 131, respectively) using the ISOCAM LW array which is a 32×32 Si:Ga photoconductor array hybridized by indium bumps (Cesarsky et al. 1996). The ISOCAM LW2 filter ($\lambda_{\rm center} = 6.75\mu$m) was used with $6''$ pixels. The field of view is $3' \times 3'$ with the use of the large field mirror.

We used the AOT (Astronomical Observation Template) CAM01. In each orbit, we took the data with six AOTs which consists of five (6×5) rasters and one (6×6) raster. The raster step was set to 6 arcsec. These six AOTs were concatenated to reduce any transient effects during the observations. Our unit integration time ($T_{\rm int}$) was 10 seconds. The data were read out 12 times at each raster point (i.e., $N_{\rm exp} = 12$). Thus the requested integration time in each orbit was 6.2 hours (= 10 × 12 × [5 × (6 × 5) + 6 × 6] seconds). The total target dedicated time (TDT) was 13.4 hours including all the overheads.

We processed the edited raw data delivered by ESA. The data reduction procedure for the ISOCAM data is basically similar to that for NIR image data; i.e., 1) dark subtraction, 2) deglitching (removal of bad pixel data due to cosmic rays, etc.), 3) flattening with skyflats, 4) sky subtraction, and 5) mosaicing (registration and coaddition).

1) Dark subtraction: We subtracted the dark currents by using the default dark frames delivered from ESA.

2) Deglitching: Infrared data taken in space are usually damaged by a large number of cosmic ray events. In our ISOCAM data, there are indeed many cosmic ray hits. Another problem is that cosmic ray events can affect the pixel response over a relatively long time scale (e.g., a few tens of minutes). Such events are referred to as "a long timescale transient". Before making skyflats, we have to remove these events from the image frames. In order to remove typical cosmic rays, we performed an iterative sigma clipping procedure with median filtering. After averaging the data stream with median filtering [the initial filter width = 3 and the i-th filter width = 3 + 2 × $(i - 1)$], we performed a sigma clipping with a threshold of 5 σ to remove bad data points. The 1 σ noise level used here is estimated by using only negative data with respect to the median data and thus is not Gaussian. This is because the positive data would be contaminated by the effect of cosmic rays. This clipping was performed until one of the following three criteria were achieved; i) $\sigma_i > \sigma_{i-1}$ where σ is the dispersion of the data stream for a particular pixel, ii) $\sigma_i < \sigma_{\rm negative}$ where $\sigma_{\rm nagative}$ is one σ noise level estimated by using negative data only, or iii) $N_{\rm clip} = 0$ where $N_{\rm clip}$ is the number of clipped data points. In most cases, several iterations satisfied one of the above criteria. The next step is to remove long timescale transients. After some trial and error, we performed this procedure by 2.5 σ clipping for median-filtered data streams (the filter width = 25). These deglitching processes typically result in $\sim$ 30 percent of the data being dropped.

3) Flattening: The flattening was performed using skyflats. For the i-th frame, we made its skyflat by using $\pm$ 72 adjacent frames. However, we did not use the frames taken both at the same raster point and at the adjacent raster ones (before and after). We also did not use the frames whose raster points were within an angular distance less than 11.4 arcsec (= the raster step size + the Airy disk size at 6.75 μm). We thus usually used about 100 frames for making skyflats.

4) Sky subtraction: The median sky (i.e., a constant) was subtracted from each frame.

5) Mosaicing: All the pointing information of the ISO satellite was recorded in the IIPH (Instrument Instantaneous Pointing History) file. The pointing data were recorded on a timescale shorter than our unit integration time (10 seconds). Therefore, we determined the sky position for each frame by averaging the pointing data during each integration. The typical pointing fluctuation in each frame was $\sigma_{\rm point} = 0.6$ arcsec. This assures that we are able to register the observed frames within an accuracy of 0.6 arcsec. Thus we divided one pixel into 10 × 10 (i.e., 100 subpixels). Then we coadded the frames by using the averaged positions of the individual frames. This procedure was made with the weighted mean average (the weight $\propto \sigma^{-2}$). We did not use any frames whose pointing accuracy was worse than 1.2 arcsec (= 2 $\sigma_{\rm point}$). About 10 percent of the total frames were dropped by this criterion. After smoothing with a boxcar av-

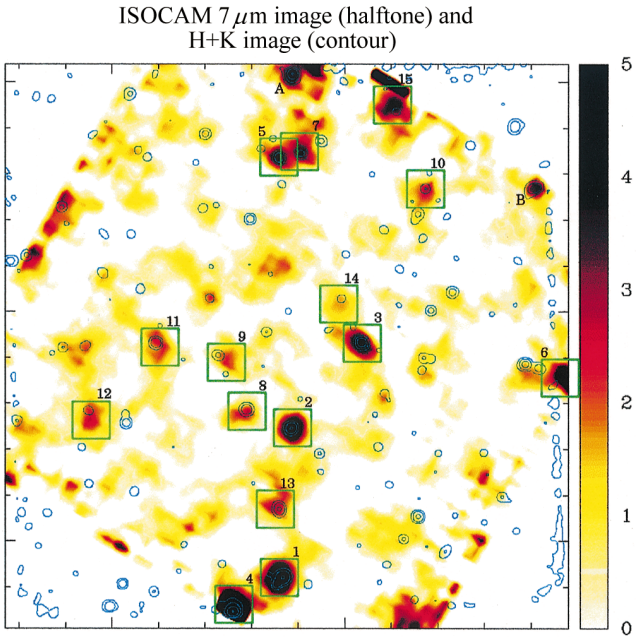

Fig. 1. The final 7 μm mosaiced image of the LH-NW area (halftone; darker is brighter). The contours show the NIR (HK) image taken with the University of Hawaii 2.2 m telescope. Although the seeing size in the NIR image is very good (FWHM $\simeq$ 0.8 arcsec), the image is blurred in order to make the comparison between the LW2 and the NIR images easier. The two sources labeled by A and B have NIR counterparts and thus they may be real sources. However, their Q parameters are less than 7 (because of the field edge), we do not include them in Table 1. North is up and east is left.

erage (the width = 9 subpixels, corresponding to the Airy disk size at 7 μm, 5.4 arcsec), we obtain the final mosaiced image.

During the course of data reduction, we computed errors (e.g., noise) in the individual pixels, giving a noise map (Sato et al. 1997). This noise map is used in the estimates of statistical significance of source detection below.

3. Results and discussion

The mosaiced 7 μm image is shown in Fig. 1 overlaid on our own NIR image[1]. The background fluctuation of the central part of the final mosaiced image is 0.09 μJy arcsec^{-2}, corresponding to a 3 σ detection limit of $\simeq$ 9.7μJy beam^{-1} (the beam size = 6$''$ $\times$ 6$''$). This limit is very close to the expected value in the ISOCAM observers manual. Thus our deep imaging observations have confirmed the very high in-flight performance of ISOCAM.

Our detection criteria are; i) counts are larger than 2 $\sigma_{\rm rms}$ (i.e., the isophotal threshold), and ii) the number of connected pixels above the threshold is more than 7. If there is more than one peak in the individual isophotes, we separated them by using FOCAS (Jarvis & Tyson 1981). In this way, we determined the center position for each source candidate. Using this center, we obtained aperture photometry for each source on the mosaiced image by using the APPHOT package in IRAF. Here we used an aperture of 12-arcsec diameter. The sky area was set to the annular region between the radii of 8 and 12 arcsec. This procedure leads to the detection of 55 sources (27 sources are above 5 $\sigma_{\rm rms}$). The true 7 μm fluxes were obtained by multiplying a factor of 2 which corrects both for the long transient response of the detector and for the effects of the point spread function (Aussel et al. 1997). Using the noise map, we also evaluate a quality parameter, Q. If the noise is distributed randomly in the frame, this corresponds exactly to the signal-to-noise ratio (S/N). Since, however, the actual noise seems to be distributed with some patterns in the frame, we use Q as a measure of S/N. Fluctuation of the noise level of a factor of two lowers the S/N by a factor of $\sqrt{2}$. Therefore, for safety, we adopt another criterion $Q > 7$ rather than $Q > 5$ in our source selection. Finally, we selected those 15 sources whose detected values are above 5 σ significance (i.e., whose scaled values are brighter than 32 μJy) with $Q > 7$. At this significance level, all the sources should be real. Although there are some probable sources which have NIR counterpart in the remaining 41 sources at 7 μm (e.g., see sources labeled by A and B in Fig. 1), we describe only the 15 sources in this *Letter*.

In Table 1, we present the basic data for the 15 sources. The objects are sorted in order of the quality parameter. It is noted that the fluxes of two sources (Nos. 3 and 13) are underestimated by the effect of high background. Those of Nos. 4, 6, and 15

Table 1. A list of 7 μm sources with high statistical significance

No.	f_ν(LW2) (μJy)	$f_\nu(K')$ (μJy)	$f_\nu(HK)$ (μJy)	R	Q
1	117.68	319.03	269.77	0.26	24.80
2	84.52	133.49	129.79	0.64	24.39
3	69.86*	372.82	405.24	0.18	23.16
4	213.06*	57.23	90.93	7.44	21.22
5	58.08	22.64	70.91	2.56	13.34
6	88.10*	NO	NO	NO	12.56
7	53.42	56.12	63.40	0.96	12.33
8	40.24	106.85	115.26	0.30	11.82
9	37.66	NC	NC	–	11.42
10	43.50	31.84	15.09	1.34	11.30
11	41.90	131.83	106.78	0.26	11.20
12	40.48	NC	NC	–	11.15
13	31.92*	150.83	160.14	0.22	9.64
14	32.34	20.88	16.65	1.54	8.95
15	64.44*	NO	5.67	NO	7.68

$R \equiv f_\nu$(LW2)$/f_\nu(K')$, Q is the quality parameter, NO: not observed, and NC: there is no NIR counterpart or the center position is significantly different ($\sim 4''$) between the LW2 and NIR images. The asterisk means an underestimate due either to high background or to proximity to the field edges.

[1] The NIR observations of the same field have been made with use of the quick infrared camera (QUIRC: Hodapp et al. 1996) attached to the University of Hawaii 88-inch telescope on Mauna Kea during the period of 1995 - 1996. We obtained K' and HK images whose limiting magnitudes are 23.30 and 24.90 in the AB magnitude system, respectively. The detailed description of these observations will be given in Sato et al. (1997).

are also underestimated because they are located near the edges of the frame. Among the 15 sources, one source (No. 6) is not observed in the NIR observations because the position angle of the LW2 image is shifted by $\sim 30^\circ$ from those of the NIR images. Among the remaining 14 sources, twelve sources have NIR counterparts while two objects (Nos. 9 and 12) have no apparent NIR counterpart [the center position is significantly different ($\sim 4''$) between the LW2 and NIR images]. The latter class of objects may be heavily reddened populations.

The observed flux ratios between LW2 and K' [$R \equiv f_\nu(\mathrm{LW2})/f_\nu(K')$] scatter from $\sim$ 0.2 to 7.4 although most of them are less than ~ 1. Since typical late-type dwarf stars show no MIR excess in their rest-frame spectra, the objects with smaller ratios (e.g., $R < 0.5$) may be Galactic stars or early type galaxies with moderate redshifts. On the other hand, starburst galaxies and active galactic nuclei usually show a MIR excess (cf. Boulade et al. 1996; Lutz 1997; Rowan-Robinson et al. 1997). Therefore the objects with the larger ratios may be such galaxies with moderate redshifts. Most of the sources discussed here have K magnitudes between 16 and 20 and thus they may have properties similar to the faint NIR galaxies studied by Cowie et al. (1996). If this is the case, the majority of our 7 μm sources may be galaxies or active galactic nuclei with $0.2 < z < 2$ (Cowie et al. 1996).

Our LW2 image of the LH-NW field is the deepest one taken so far with ISOCAM. Note that our image is 2.5 times deeper than that of Hubble Deep Field taken by Rowan-Robinson et al. (Goldschmidt et al. 1997; Oliver 1997; Rowan-Robinson et al. 1997). Therefore, we believe that our ISOCAM LW2 deep survey project will provide a new frontier in the study of high-z forming galaxies.

Acknowledgements. We would like to thank all the staff of the Infrared Space Observatory around the world. In particular, we would like to thank Martin Kessler, Catherine Cesarsky, and David Elbaz for their encouragement. Special thanks are due to the ISOCAM team. We also thank ISAS, NASA, the Ministry of Education, Science, Culture, and Sports of Japan and the Japanese ISO consortium, in particular, Takashi Tsuji, and Toshihiko Tanabe for their kind support. YS was supported by JSPS.

References

Arimoto N., Yoshii Y., 1987, A&A 173, 23
Aussel H., Elbaz D., Starck J.L., Cesarsky C.J., 1997, in Extragalactic Astronomy in the Infrared, eds. G. Mamon, T. Thuan, J. TranhVan (Gif-sur-Yvette: Ed. Frontieres) (in press)
Boulade O., Sauvage M., Altieri B., et al. 1996, A&A 315, L85
Cesarsky C.J., Abergel A., Agnese P., et al., 1996, A&A 315, L32
Cowie L. L. 1988, in The Post-recombination Universe, ed. N. Kaiser A. Lanzeby (Dordrecht: Kluwer), 1
Cowie L.L., Gardner J.P., Hu E.M., et al., 1994, ApJ 434, 114
Cowie L.L., Gardner J.P., Lilly S.J., McLean I.S., 1990, ApJ 360, L2
Cowie L.L., Hu E.M., Songaila A., 1995, Nat 377, 603
Cowie L.L., Songaila A., Hu E.M., Cohen J.G., 1996, AJ 112, 839
Djorgovski S., Soifer B.T., Pahre M.A., et al., 1995, ApJ 438, L13
Ellis R.S., 1997, ARA&A (in press)
Fukugita M., Hogan C.J., Peebles P.J.E., 1996, Nat 381, 489
Goldschmidt P., Oliver S., Serjeant S., et al. 1997, MNRAS 289, 465
Hodapp K.-W., Hora J.L., Hall D.N.B., et al., 1996, New Astronomy 1, 177
Jahoda K., Lockman F.J., McCammon D., 1990, ApJ 354, 184
Jarvis J.F., Tyson J.A., 1981, AJ 86, 476
Kessler M.F., Steinz J.A., Anderegg M.E., et al., 1996, A&A 315, L27
Lanzetta K.M., Yahil A., Fernandes-Soto A., 1996, Nat 381, 759
Lockman F.J., Jahoda K., McCammon D., 1986, ApJ 302, 432
Lutz D., 1997, ISO INFO No.10
Ohta K., Yamada T., Nakanishi K., et al., 1996, Nat 382, 426
Oliver S., 1997, in Taking ISO to the Limits: Exploring the Faintest Sources in the Infrared (ESA), Section VI
Omont A., Petitjean P., Guilloteau S., et al., 1996, Nat 382, 428
Rowan-Robinson M., Mann R.G., Oliver S.J., et al., 1997, MNRAS 289, 490
Sato Y., Cowie L.L., Taniguchi Y., et al., 1997, in preparation
Steidel C.S., Giavalisco M., Dickinson M., Adelberger K.L., 1996a, AJ 112, 352
Steidel C.S., Giavalisco M., Pettini M., Dickinson M., Adelberger K.L., 1996b, ApJ 462, L17
Taniguchi Y., Okuda H., Wakamatsu K., et al., 1994, in Evolution of the Universe and Its Observational Quest, ed. K. Sato (Universal Academy Press; Tokyo), 545
Taniguchi Y., Kawara K., Okuda H. et al. 1997, in Taking ISO to the Limits: Exploring the Faintest Sources in the Infrared (ESA), Section VI
Tyson J. A. 1988, AJ, 96, 1
Williams R. E., Blacker B., Dickinson M., et al. 1996, AJ, 112, 1335

This article was processed by the author using Springer-Verlag LaTeX A&A style file *L-AA* version 3.